

Mechanical anchorage and peri-implant bone formation of surface-modified zirconia in minipigs

Henning Schliephake¹,
Thomas Hefti², Falko Schlottig²,
Philippe Gédet³ and Henning Staedt¹

¹Department of Oral and Maxillofacial Surgery, George-Augusta-University, Göttingen, Germany; ²Thommen Medical, Waldenburg, Switzerland; ³MEM Research Center, University of Bern, Bern, Switzerland

Schliephake H, Hefti T, Schlottig F, Gédet P, Staedt H. Mechanical anchorage and peri-implant bone formation of surface-modified zirconia in minipigs. *J Clin Periodontol* 2010; 37: 818–828. doi: 10.1111/j.1600-051X.2010.01549.

Abstract

Aim: To test the hypothesis that peri-implant bone formation and mechanical stability of surface-modified zirconia and titanium implants are equivalent.

Materials and Methods: Twelve minipigs received three types of implants on either side of the mandible 8 weeks after removal of all pre-molar teeth: (i) a zirconia implant with a sandblasted surface; (ii) a zirconia implants with a sandblasted and etched surface; and (iii) a titanium implant with a sandblasted and acid-etched surface that served as a control. Removal torque and peri-implant bone regeneration were evaluated in six animals each after 4 and 13 weeks.

Results: The titanium surface was significantly rougher than both tested zirconia surfaces. Mean bone to implant contact (BIC) did not differ significantly between the three implant types after 4 weeks but was significantly higher for titanium compared with both zirconia implants after 13 weeks ($p < 0.05$). Bone volume density (BVD) did not differ significantly at any interval. Removal torque was significantly higher for titanium compared with both zirconia surfaces after 4 and 13 weeks ($p < 0.001$). The sandblasted and etched zirconia surface showed a significantly higher removal torque after 4 weeks compared with sandblasted zirconia ($p < 0.05$); this difference levelled out after 13 weeks.

Conclusions: It is concluded that all implants achieved osseointegration with similar degrees of BIC and BVD; however, titanium implants showed a higher resistance to removal torque, probably due to higher surface roughness.

Key words: animal study; osseointegration; surface roughness; titanium; zirconia

Accepted for publication 9 January 2010

Yttria-stabilized zirconia ceramic (Y-TZP) has been extensively described in the literature (for a review, see Piconi & Maccauro 1999) and is currently applied in different fields of dentistry. In implant dentistry, it is used as a material for ceramic abutments and frameworks due

to its high fracture strength, its low affinity to bacterial colonization and its favourable aesthetic characteristics (Rimondini et al. 2002, Groessner-Schreiber et al. 2004, Canullo 2007, Kokubo et al. 2007, Rompen et al. 2007, Sundh & Sjögren 2008). These characteristics have also made zirconia attractive for the fabrication of endosseous implants in order to avoid unfavourable discoloration due to titanium shining through thin peri-implant soft tissues (Jung et al. 2007, Oliva et al. 2007, Park 2007). Only recently has zirconia been identified as a potential material for endosseous implants; however, clinical

studies supportive of this kind of use are still lacking (Andreietelli et al. 2009).

Surface characteristics have been reported to affect osseointegration of zirconia in a manner comparable to titanium in that removal torque was significantly lower for machined zirconia surfaces compared with rough surface modifications. Nevertheless, zirconia surfaces with a roughness of S_a of $0.56 \mu\text{m}$ still exhibited significantly lower removal torque values than sandblasted and acid-etched titanium surfaces with an S_a of $1.15 \mu\text{m}$ (Gahlert et al. 2007). In contrast, zirconia and titanium implants with simi-

Conflict of interest and source of funding statement

The authors declare that there are no conflicts of interest in this study. This study was supported by a grant from Thommen Medical.

lar surface roughness ($S_a = 1.24$ and $1.30 \mu\text{m}$, respectively) had reached comparable torque-out values (Sennerby et al. 2005).

Interface analysis with respect to bone to implant contact (BIC) has shown that BIC of zirconia implants was comparable to titanium surfaces in implants with a custom-made root form geometry in primates (Kohal et al. 2004). Moreover, BIC to zirconia implants also remained high under medium-term functional loading in an experimental setting (Akagawa et al. 1993, 1998). So far, animal studies of rough surface modifications of zirconia for dental implants have been performed on sandblasted implant surfaces (Gahlert et al. 2007) and on zirconia surfaces with an added porous layer (Sennerby et al. 2005) (for a review, see Wenz et al. 2008, Andreiottelli et al. 2009). Additional etching to create a micro-rough surface structure with pits and grooves and to remove corundum contamination resulting from sandblasting (Aparicio et al. 2003) could further improve the rough surface characteristics as it has been reported for titanium but has not been tested as yet in vivo with zirconia implants. Additional research is thus desirable to iden-

tify the surface characteristics of zirconia implants that can achieve bone anchorage comparable to rough titanium surfaces that are currently in clinical use.

It was, therefore, the aim of the present in vivo study to test the hypothesis that peri-implant bone formation and mechanical anchorage in the bone adjacent to zirconia implant surfaces modified by sandblasting or sandblasting and etching is equivalent to well-documented sandblasted and acid-etched titanium implant surfaces.

Materials and Methods

Implant design/surface characteristics

A total of 72 screw-type implants with the identical SPI[®] ELEMENT geometry were used (4.2 mm diameter and 8 mm length of the endosseous part with a conical machined neck of 1 mm height and 4.5 mm upper diameter) (Thommen Medical AG, Waldenburg, Switzerland). All implants had an internal hex connector for force transmission during insertion and torque-out measurements and allowed for submerged healing. Implants were manufactured from yttria partially stabilized zirconia medical grade

(Y-TZP) and titanium grade 4, respectively. Three types of rough surface modifications were applied to the endosseous part of the implants for testing:

Group 1: zirconia with a sandblasted surface. Sandblasting was performed with corundum (grain size 105–150 μm) at 4 bar (Fig. 1a).

Group 2: zirconia with a sandblasted and etched surface. Sandblasting was performed as described above with subsequent immersion in an alkaline salt bath (Fig. 1b).

Group 3: titanium with a sandblasted and acid-etched surface, a surface known to perform osseointegration (Bornstein et al. 2005), which served as a control (Fig. 1c).

Both implants and disc-shaped samples for evaluation of surface topography were prepared and treated in an identical manner.

Surface topography

Disc-shaped samples of the tested materials and surface modifications were sputtered with gold and subjected to scanning electron microscopic (SEM)

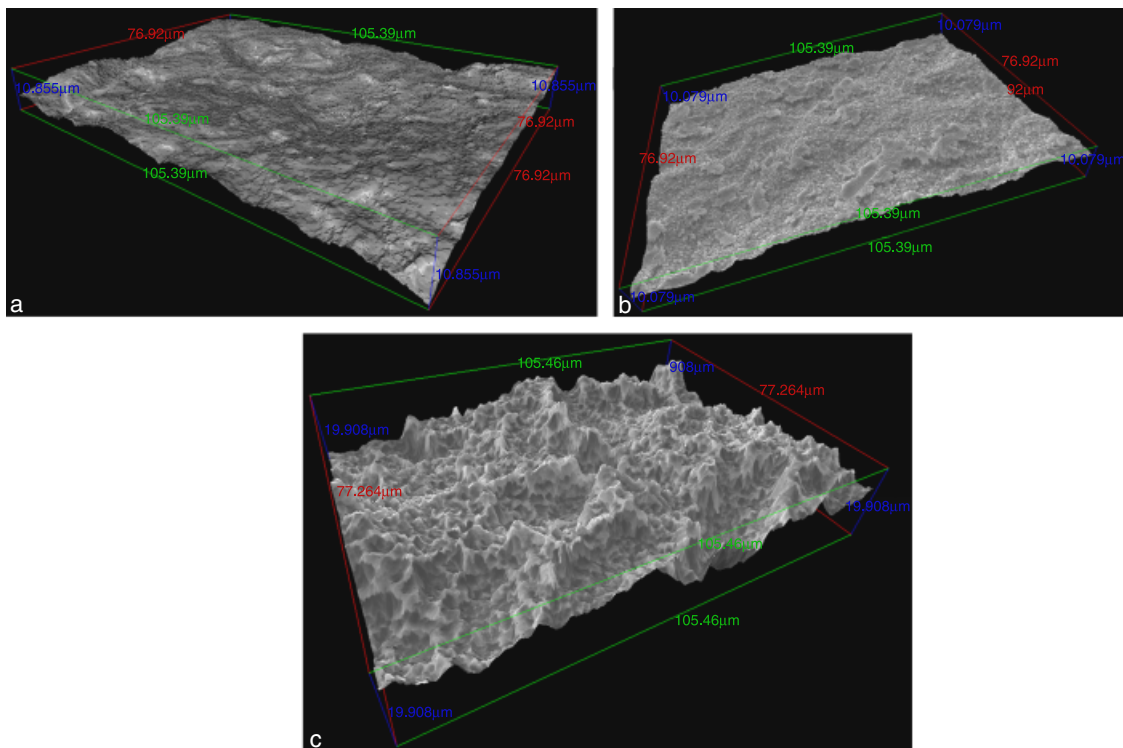


Fig. 1. (a) Stereo-scanning electron microscopic (SEM) image showing the sandblasted zirconia surface (group 1) with a rather smooth surface (original magnification $\times 1.000$). (b) Stereo-SEM image showing the sandblasted/etched zirconia surface (group 2) with additional microroughness (original magnification $\times 1.000$). (c) Stereo-SEM image showing the sandblasted and acid-etched titanium surface (group 3) with considerably higher macroroughness but also more pronounced microstructural pits and grooves (original magnification $\times 1.000$).

analysis (Zeiss MA 25, Zeiss, Obercochen, Germany). Disc-shaped samples were used instead of original implants to facilitate the measurements. Stereoscopic pictures were generated using SEM projections with a $\times 1000$ magnification that were 6° apart. The three-dimensional (3D) images of the surface topography were calculated using MeX V5.1 software (Alicona, Grambach, Austria). A 3D-wavelength-dependent roughness measurement was applied using the common cut-off method (Whitehouse 1994). This method has been reported previously for the description of implant surfaces (Wieland et al. 2001). S_a values were calculated for each surface modification with two different cut-off lengths λ_c , which were $\lambda_{c1} = 580 \mu\text{m}$ and $\lambda_{c2} = 5 \mu\text{m}$, respectively. Areas of $341 \times 232 \mu\text{m}$ in five surface samples of each group were measured. The S_a values obtained for $\lambda_{c1} = 580 \mu\text{m}$ represented the range of macroroughness of the specimen surface whereas those obtained for $\lambda_{c2} = 5 \mu\text{m}$ represented microroughness in the sub-micron range. 3D-wavelength-dependent measurements were used instead of optical surface profilometry using a light interferometer because the xy resolution of the latter is limited by the wavelength of visible light (approximately 300 nm) and the surface features of both etched surfaces were below this limit.

Surface chemistry

Assessment of surface chemistry was performed on implants as produced for the animal experiments. Implants were taken directly out of the ampoule and placed into the vacuum chamber of the XPS device. A Kratos Axis Nova (Kratos Analytical, Manchester, UK) was used with a monochromatic X-ray source (AlK α) with an accelerating voltage of 15 kV and an emission current of 15 mA. The measured area was $700 \times 300 \mu\text{m}$; two positions were measured per sample. The quantitative evaluation of the chemical composition of the surface was performed using the software casaXPS (V2.3.12, Casa Software Ltd., Teignmouth, UK).

Study design and animal model

The pig mandible has been established as a model for implant research in recent years (Fuerst et al. 2003, Zechner et al. 2003, Fuerst et al. 2004, Stadlinger et al. 2007). The study was performed on 12

skeletally mature female minipigs (average weight 31.3 kg). On either side of the mandible, one implant of each type was placed (six implants per animal). A split-mouth design with rotating positions on either side of the mandible was developed before surgery to ensure a homogeneous distribution of all groups. The position of each implant type in the mandible was rotated by one position between the animals. At the end of the observation period, one side of the mandible was assigned to histological evaluation; the remaining half was used for biomechanical testing.

Surgical procedure

In a first surgical series, all deciduous pre-molar teeth of the mandibles were removed. After 13 weeks, the erupted permanent pre-molars were removed. Eight weeks later, the implants were placed (first author, H. S.). At this time, the animals were 19.1 months of age on average and considered skeletally mature. The alveolar crest was re-exposed through a buccal incision after elevation of a lingually based mucoperiosteal flap. Implant sites were prepared

in the edentulous area using spiral drills with increasing diameter and a screw tap. Depending on the anatomical situation, the implants were placed at a distance of 2.0–3.0 mm to each other. The two zirconia test implants and the titanium control implant were inserted on both sides of the mandible. The implant necks were placed slightly subcrestal (Fig. 2a). Care was taken not to perforate the cortical bone on either side of the crest and to preserve a bone thickness of at least 1 mm all around the implants' circumference. The terminal insertion torque was approximately 55 N cm. During insertion, the walls of the hexagonal connector broke at the neck of seven implants at insertion torques of $> 55 \text{ N cm}$ (Fig. 2b), leaving the surface-modified part intact. After placement of titanium cover screws (control implants) and polyetheretherketone (PEEK) caps (zirconia implants) (Fig. 2c), the wounds were closed using resorbable polyglactin sutures. In implants with broken connector walls, no PEEK caps were used. After 4 and 13 weeks, the mandibles of the animals were retrieved after sacrifice in deep sedation using an intra-cardial injection

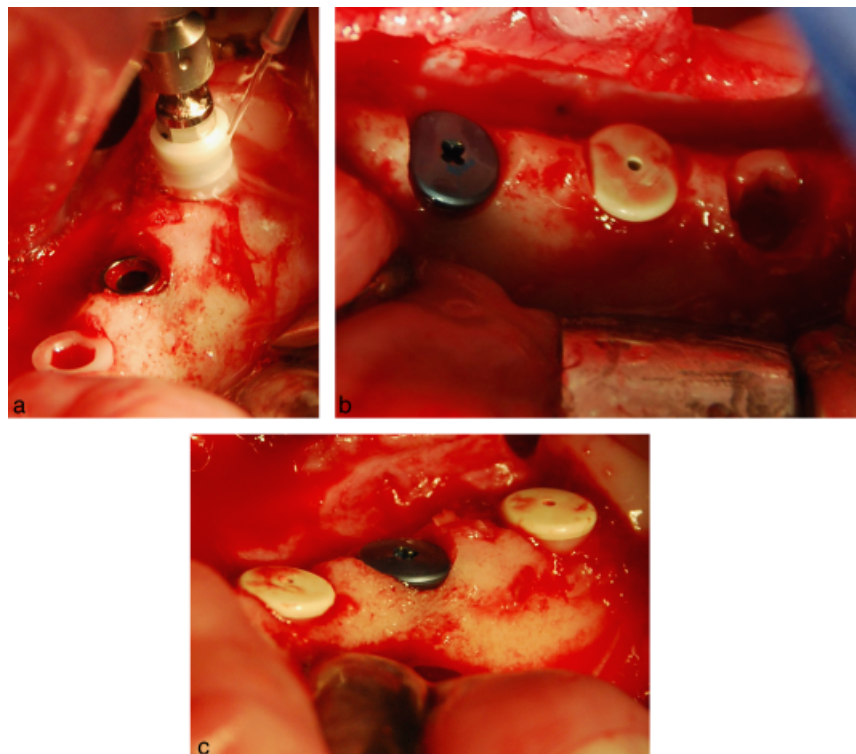


Fig. 2. (a) Zirconia implant with inserted connector during placement. (b) Implants after placement. The titanium implants received a commercially available cover screw whereas the zirconia implants were covered with a polyetheretherketone cap. (c) Implants after placement; note the posterior implant has lost large parts of its connector walls during the terminal increase in insertion torque.

of T61[®] (Intervet, Unterschleißheim, Germany). The mandibles were divided in the midline and implants on one side of the mandibles of six animals each were subjected to mechanical testing. Only blocks with intact connector walls were chosen for mechanical testing. The opposite halves of the mandibles were used for histologic and histomorphometric evaluation. As broken connector walls did not reach into the area of the modified rough surface section, all implants in these parts of the mandibles were available for histological assessment.

Mechanical testing

All soft tissue was removed from the bone blocks. The cut mandibles, containing three implants, were wrapped in gauze soaked with an isotonic NaCl solution and tightly packed in plastic bags to prevent drying during transportation. Samples were stored for a maximum of 36 h at 7°C until testing.

For handling reasons and to provide appropriate temperature isolation, each bone bloc was embedded into dental plaster (GC Fujirock, GC Europe NV, Leuven, Belgium) with a curing time of only a few minutes.

All removal torque tests were performed on a biaxial servo-hydraulic material testing machine (MTS Mini Bionix 858, Eden Prairie, MN, USA) equipped with an axial-torsional load transducer (MTS 662.20D-04, MTS Systems, Eden Prairie, MN, USA) to measure and record the removal torque. The bone–dental–plaster complex was attached through the implant hexagon socket via a modified adaptor (Thommen Medical AG) to the machine flange, which itself is fixed to the plunger of the actuator. This whole complex was then lowered into an aluminium container, which was slightly larger than the dental plaster complex and provided some clearance between the container walls. By filling the clearances with a low-melting metal alloy (Sonderweichlot, 47° eutektisch, Felder Löttechnik, Oberhausen, Germany), a rigid fixation of the specimen in the machine was obtained after solidification of the alloy. This procedure guaranteed an in-axis alignment of the implant axis to the actuator rotational axis. The interface between the adaptor and the machine flange was designed in such a way that the adaptor was vertically unconstrained to eliminate any axial loading on the implant, but at the same time allowing

transmission of the applied torque to the implant. After solidification of the alloy, the removal torque test was started by rotating the implant counter clockwise at a rate of 0.5°/s to an angle of 30°. Angle and torque data were simultaneously collected at a sampling rate of 20 Hz. After completed testing, the embedding alloy was melted to remove the bone–dental–plaster complex from the aluminium container. The same test procedure, as described before, was repeated for the remaining two implants of the bone bloc. During the entire testing, the specimens were sprayed frequently with saline solution to avoid drying of the bone.

The torque–rotation–angle curve obtained was first smoothed with in-house developed software before being analysed to determine the removal torque failure point. For specimens with a clear peak, followed by an immediate drop in torque, the failure point (Ncm) was defined as the peak on the removal torque curve. In cases where the curve constantly increased or showed a plateau, the failure point was defined as follows: by constructing a straight line parallel to the initial slope of the torque–rotation–angle curve with an offset of 0.72°, which corresponds to 0.2% of a full rotation, the intersection point of this shifted parallel line with the original torque–rotation–angle curve could be defined as the failure point (Fig. 3).

Histologic processing and evaluation

For histologic evaluation, the mandibular segments were fixated in 4% buffered formalin immediately after retrieval. The implants were located radiographically

and the mandibular bone was then separated using a diamond coated saw (Exakt, Norderstedt, Germany) into segments that contained one implant each. The individual implants with surrounding bone were embedded into methylmethacrylate. Consecutive thick sections (thickness approximately 100–150 µm) of the embedded specimens were fabricated parallel to the long axis of the implants in the bucco-oral direction and ground to a thickness of approximately 70 µm (Exact). The resulting specimens were surface stained using toluidine blue and alizarine–methylene blue.

The specimens were evaluated by registering active bone formation showing osteoid and osteoblast seams as well as osteoclastic resorption and the nature of the BIC. Histomorphometry was performed using a video camera (Sony 3CCD, Berlin, Germany) to record images at ×50 magnification. The images were digitized (Axiophot-System, Zeiss) and the BIC was measured by counting all pixels of the implant contour occupied by bone. BIC was expressed as the percentage of the perimeter of the implant cross section. The volume density of the newly formed peri-implant bone (BVD) was assessed by calculating the percentage of the surface area inside the screw threads. The area of evaluation was defined by placing a tangent line on the thread tips and counting all pixels between this tangent line and the implant contour within the groove. In case of fractured connector walls, the available implant contour was evaluated. Evaluation was performed by an examiner (H. S.) blinded to the surface modification of the zirconia implants.

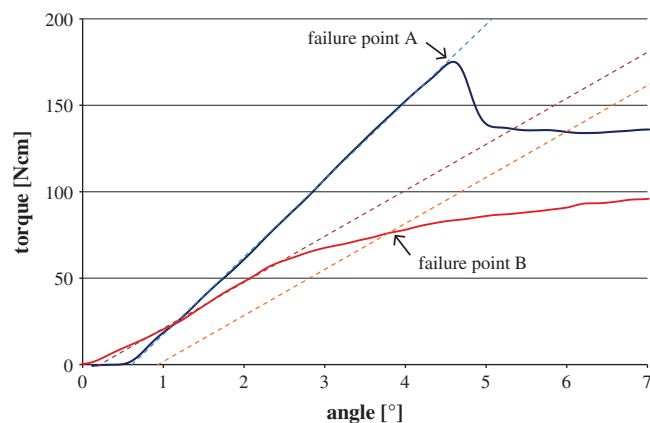


Fig. 3. Definition of the failure point in the torque-out curves. If a clear peak could be identified, this is defined as the failure point A. Where no clear peak could be determined, the failure point was defined by constructing a parallel line to the initial slope with an offset of 0.2%. The intersection point of this straight line with the measured data are defined as the failure point B.

Statistical evaluation

Surface topography measurement

The mean values of the surface roughness of the three surfaces were statistically analysed using Student's *t*-test. Differences were considered significant at a level of $p < 0.01$.

Mechanical testing

Single measurements were defined as outliers according to the procedure proposed by Grubbs (1969). The mean values of the removal torque results were statistically analysed using Student's *t*-test. Single factors like surface type and healing period were evaluated. Differences were considered significant at a level of $p < 0.05$.

Histomorphometric evaluation

Mean values were calculated for each implant and for each group of implants. Differences in the group mean values were analysed for statistical significance using Friedman's tests within the groups of each observation interval. When differences between the three different surfaces were significant, pairwise testing using Wilcoxon's tests were performed. Kruskal-Wallis tests were used for comparisons between the two observation intervals. Differences were considered significant if $p < 0.05$.

Results

Surface topography

The SEM images showed that the sandblasted zirconia surface exhibited a macrorough topography in the range of 10–20 μm ; microroughness in the sub-micron range was not appreciable (Fig. 1a). On the sandblasted and etched zirconia surface this topography was preserved; however, additionally, microroughness in the submicron range was visible. The etching process had revealed a surface structure with micro-roughness in the size range of single grains of the bulk material, which is around 0.35 μm (Fig. 1b). The reference titanium surface showed the widely described titanium surface, which is obtained through sandblasting and acid etching. The sandblasting yielded a roughness in the range of 10–30 μm ; the additional etching conferred a pronounced microroughness with pits and grooves. The roughness of the etched

titanium surface appeared to be more distinct than the zirconia surfaces with respect to both the micron and the submicron range. The surface features in the submicron range, obtained through etching, appeared to be sharper on titanium than on zirconia (Fig. 1c).

These surface features are reflected quantitatively in the wavelength-dependent roughness values presented in Table 1. The S_a value calculated with $\lambda_{c1} = 580 \mu\text{m}$ describes the overall roughness mainly influenced by the sandblasting, whereas the S_a calculated with the cut-off length $\lambda_{c2} = 5 \mu\text{m}$ describes the roughness in the wavelength below 5 μm , in this case mainly influenced by the etching. The overall roughness ($\lambda_{c1} = 580 \mu\text{m}$) of both zirconia surfaces was significantly lower ($p < 0.01$) compared with titanium. However, the etched zirconia surface showed a significantly higher ($p < 0.01$) microroughness ($\lambda_{c2} = 5 \mu\text{m}$) than the blasted surface. The titanium surface showed a significantly higher microroughness than both zirconia surfaces ($p < 0.01$).

Surface chemistry

The results of the XPS analysis are summarized in Table 2. As expected, the chemical composition of the implant surface showed mainly zirconia and titanium oxide, respectively. On the sandblasted zirconia surfaces, residues

Table 1. Wavelength-dependent roughness values S_a (μm) for all surfaces: sandblasted zirconia (group 1), sandblasted and etched zirconia (group 2), sandblasted and acid-etched titanium (group 3)

	$\lambda_{c1} = 580 \mu\text{m}$		$\lambda_{c2} = 5 \mu\text{m}$	
	SD	SD	SD	SD
Group 1	0.188	0.006	0.968	0.069
Group 2	0.212	0.010	1.162	0.086
Group 3	0.342	0.005	2.578	0.035

Obtained with two different cut-off lengths describing the roughness in the macro-scale ($\lambda_{c1} = 580 \mu\text{m}$) and the micro-scale ($\lambda_{c2} = 5 \mu\text{m}$).

Table 2. XPS analysis of the sample surfaces: sandblasted zirconia (group 1), sandblasted and etched zirconia (group 2), sandblasted and acid-etched titanium (group 3) chemical composition of the surface (XPS) (at.%)

	Zr	Ti	O	C	Y	Al	N	F	P	Zn
Group 1	10.5	–	51.1	22.8	0.7	14.5	–	–	0.6	–
Group 2	18.0	–	53.2	26.1	1.2	–	–	–	1.4	0.2
Group 3	–	21.7	52.2	23.2	–	–	0.6	2.3	–	0.2

of alumina blasting particles were detectable. These particles partly masked the zirconia surface, leading to a lower detection of zirconia on the sandblasted surface. The corundum particles were apparently completely removed by the etching process and were no longer seen on the sandblasted and etched zirconia surfaces as indicated by the lack of an aluminium signal. Also, no residues of the etching process were found on the etched zirconia surface. The reference surface showed a clean titanium oxide surface, again without residues of the blasting and etching process.

In vivo experiments

Healing was uneventful in all animals. All implants were available for evaluation. No signs of infection were registered at the time of implant retrieval.

Mechanical testing

Two samples had to be excluded from the evaluation. One titanium implant from the 13-week time point was excluded because it was defined as an outlier; the second specimen, a sandblasted and etched zirconia implant from the 4-week time point, was excluded because of technical difficulties during the biomechanical testing.

After 4 weeks, the sandblasted and etched zirconia surface performed significantly better ($p < 0.05$) than the zirconia with the sandblasted-only surface (55.9 versus 111.8 N cm). However, the reference titanium surface performed significantly better than both zirconia surfaces (244.5 N cm) ($p < 0.001$), respectively. After 13 weeks, the overall picture had changed in that the sandblasted zirconia surface had caught up with the etched zirconia surface (99.4 versus 100.3 N cm). This increase from week 4 to week 13 for sandblasted zirconia was significant ($p < 0.05$). However, the mean removal torque values of both zirconia surfaces were still significantly lower than that of

Table 3. Removal torque values after 4 and 13 weeks for the different surfaces

Implant surface	Removal torque (N cm)	
	week 4	week 13
Sandblasted zirconia	55.9 ± 18.4	99.4 ± 30.9
Sandblasted and etched zirconia	111.8 ± 42.4	100.3 ± 47.0
Sandblasted and etched titanium	244.5 ± 34.9	221.9 ± 27.1

$n = 6$ for all groups, except sandblasted and etched zirconia (4 weeks) and sandblasted and etched titanium (12 weeks), where $n = 5$.

the titanium surface (221.9 N cm) ($p < 0.001$). The removal torque of sandblasted and etched zirconia surfaces as well as the control titanium surface did not change significantly between week 4 and week 13 (Table 3).

The two zirconia surfaces showed a distinct difference in the torque–rotation-angle curve (Fig. 3), where all sandblasted and etched samples showed a clear peak, followed by an immediate drop (A), whereas none of the sandblasted zirconia implants showed a clear failure point (B); this was observed for both time points. All titanium implants showed both types of curves at both time points.

Histologic results/4-week healing period

Implants with sandblasted zirconia surfaces (group 1) showed peri-implant bone regeneration that was slowly approaching the implant surface. BIC was established in small areas interrupted by portions of well-vascularized soft tissue or by a non-mineralized tissue layer between the newly formed bone tissue and the implant surface, whereas others exhibited a more consolidated BIC rate (Fig. 4a and b). The newly formed bone inside the threads was intensely re-modelled. Bone formation adjacent to zirconia implants with sandblasted and etched surfaces (group 2) showed comparable features of early BIC through thin trabeculae approaching the implant from a distance of some 50 μ m in some areas (Fig. 4c and d). Inside the threads, bone tissue was subject to intense re-modelling. The bone formation adjacent to the sandblasted and acid-etched titanium implants was clearly more osteoconductive, producing thin layers of bone on the implant surface (Fig. 4e) and filling many threads by bone formation along the thread surface (Fig. 4f). Close-up views showed intense re-modelling activity with commencing osteon formation.

Histologic results/13-week healing period

After 13 weeks, zirconia implants with sandblasted surfaces (group 1) still exhibited areas of commencing BIC through osteoconductive bone growth on the surface (Fig. 5a). There were also areas with a denser bone structure inside the threads that was actively remodelled (Fig. 5b). Implants from group 2 with sandblasted and etched zirconia surfaces also showed some areas with thinner layers of bone tissue immediately adjacent to the implant surface. In particular, individual thread tips appeared to show less intense BIC while others had extensive BIC (Fig. 5c). The control titanium implants presented a mature peri-implant bone structure with extensive coverage of the implant surface. Bone re-modelling had decreased compared with the 4-week features (Fig. 5d).

Histomorphometric results/4-week healing period

After 4 weeks, zirconia implants with sandblasted surfaces exhibited a mean BIC rate of 57.5% (SD 14.3). This was not significantly lower than the mean BIC of zirconia implants with a sandblasted and etched surface (66.7%, SD 15.8) or the BIC value of titanium implants with a sandblasted and etched surface (69.3%, SD 17.1). Bone volume density (BVD) was the highest in zirconia implants with sandblasted and etched surfaces (72.1%, SD 21.6), however, again without statistically significant differences compared with the values of the sandblasted zirconia implants (61.3%, SD 12.4) and the control titanium implants (65.3%, SD 11.3) (Fig. 6a).

Histomorphometric results/13-week healing period

After 3 months, the mean BIC value had decreased in the group of zirconia

implants with a sandblasted surface to 54.6% (SD 17.6) as well as in the group of sandblasted and etched zirconia implant surfaces (57.6%, SD 23.7). Again, the highest mean BIC values were found with titanium sandblasted and etched surfaces, with 78.9% (SD 5.8). Differences between the titanium surface and both zirconia surfaces were significant (sandblasted: $p = 0.024$; sandblasted and etched: $p = 0.046$). Differences between the two zirconia surfaces were not significant. The mean BVD within the threads of the sandblasted zirconia surface was 70.9% (SD 18.5), which was not significantly different from zirconia implants with sandblasted and etched surfaces (70.7%, SD 18.5) or from control titanium implants with sandblasted and acid-etched surfaces (80.5%, SD 14.4) (Fig. 6b).

The differences in the mean BIC and mean BVD between 4 and 13 weeks were not significant for all surfaces.

Discussion

In the present study, the performance of experimental zirconia implants with two different surfaces was compared with a reference titanium surface on implants of identical geometry. It could be shown that surface-modified zirconia implants had reached similar values of BIC and peri-implant bone density (BVD) compared with sandblasted and acid-etched titanium implants after 4 weeks, whereas a significant difference was found after 13 weeks, where sandblasted and etched titanium surfaces had shown significantly higher BIC than the two tested zirconia surfaces.

The histomorphometric results of BIC values after 4 weeks in the present study were in the same order of magnitude as in previous reports without a significant difference between zirconia and titanium implants (Akagawa et al. 1993, 1998, Kohal et al. 2004, Sennerby et al. 2005). It is interesting to note that the level of both BIC and BVD values does not vary grossly throughout the literature, although the experimental models and the characteristics of the individual surface modifications were distinctly different in all available reports: Kohal and colleagues had compared custom-made implants produced from CAD/CAM data of extracted teeth, whereas Sennerby and colleagues had evaluated zirconia implants with porous sintered zirconia coatings of different

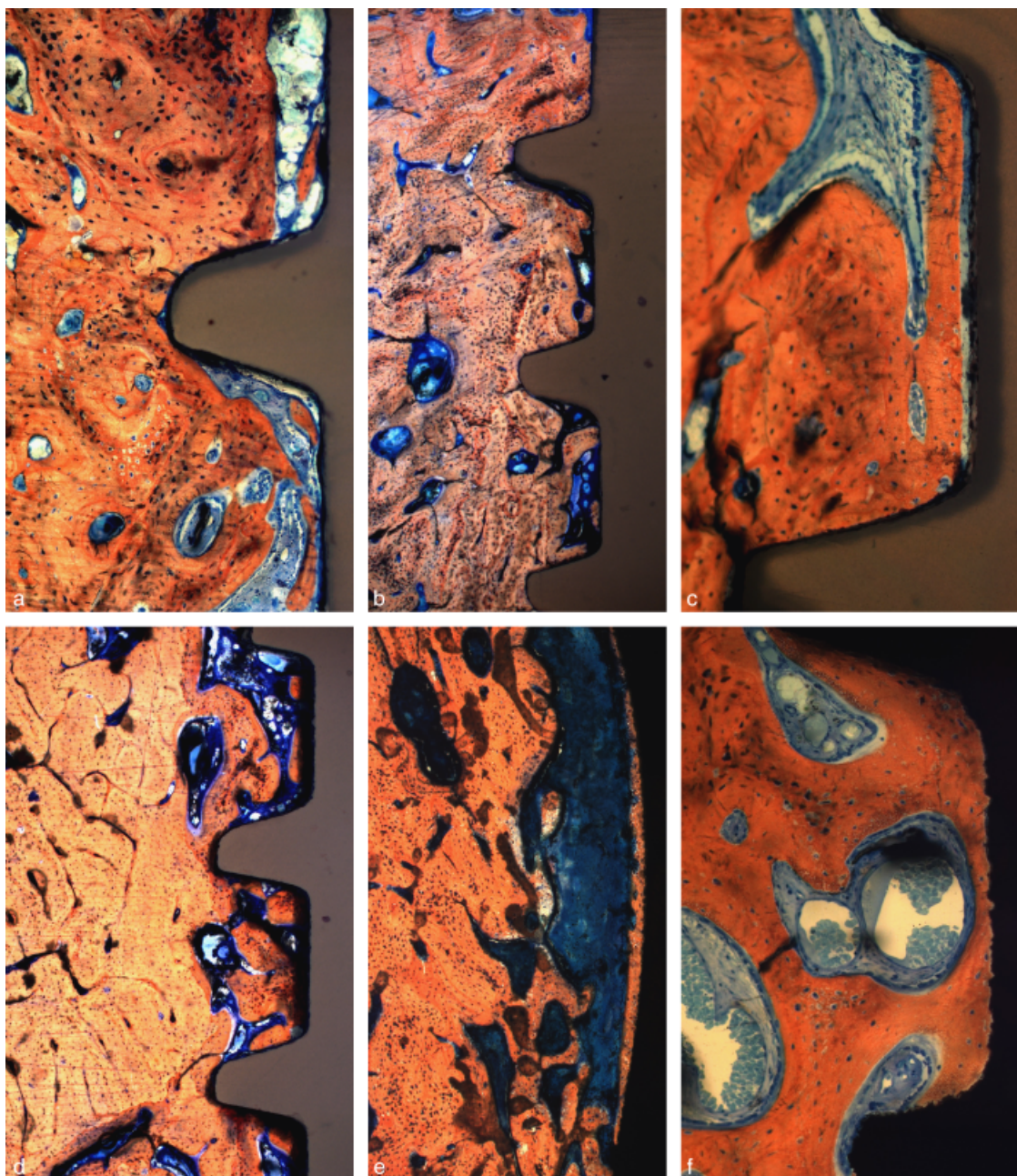


Fig. 4. (a) Micrograph showing bone regeneration after 4 weeks next to a sandblasted zirconia implant surface with small spots of bone contact and fibrous/vascular tissue in between. (alizarine–methylene blue, original magnification $\times 100$). (b) Micrograph showing consolidated bone regeneration after 4 weeks next to a sandblasted zirconia implant (alizarine–methylene blue, original magnification $\times 50$). (c) Micrograph showing commencing bone regeneration after 4 weeks that moved along the sandblasted and etched surface of a zirconia implant. Note the non-mineralized area between bone and implant surface (alizarine–methylene blue, original magnification $\times 150$). (d) Micrograph showing bone formation with a lower bone contact rate due to intervening soft tissue (alizarine–methylene blue, original magnification $\times 50$). (e) Micrograph showing extensive osteoconductive bone formation after 4 weeks on the surface of an sandblasted and acid-etched titanium implant (alizarine–methylene blue, original magnification $\times 150$). (f) Micrograph showing high bone formed in the thread of a sandblasted and acid-etched titanium implant. Bone has been laid down on the surface and active osteoblast seams are visible around accompanying vessels (alizarine–methylene blue, original magnification $\times 150$).

roughnesses and oxidized titanium surfaces. The overall surface roughness of the implants in the Sennerby study had varied considerably between the two modified zirconia surfaces and the surfaces were different in morphology from

the two zirconia surfaces in the present study.

The rather uniform BIC values regardless of the implant surface and experimental model are difficult to explain. In vitro data with respect to

material effects and surface modifications of zirconia are rather inconsistent. Cultures of osteoblast-like cells have exhibited up-regulated BMP4 and BMP7 genes in cell cultures on titanium disks compared with zirconia surfaces

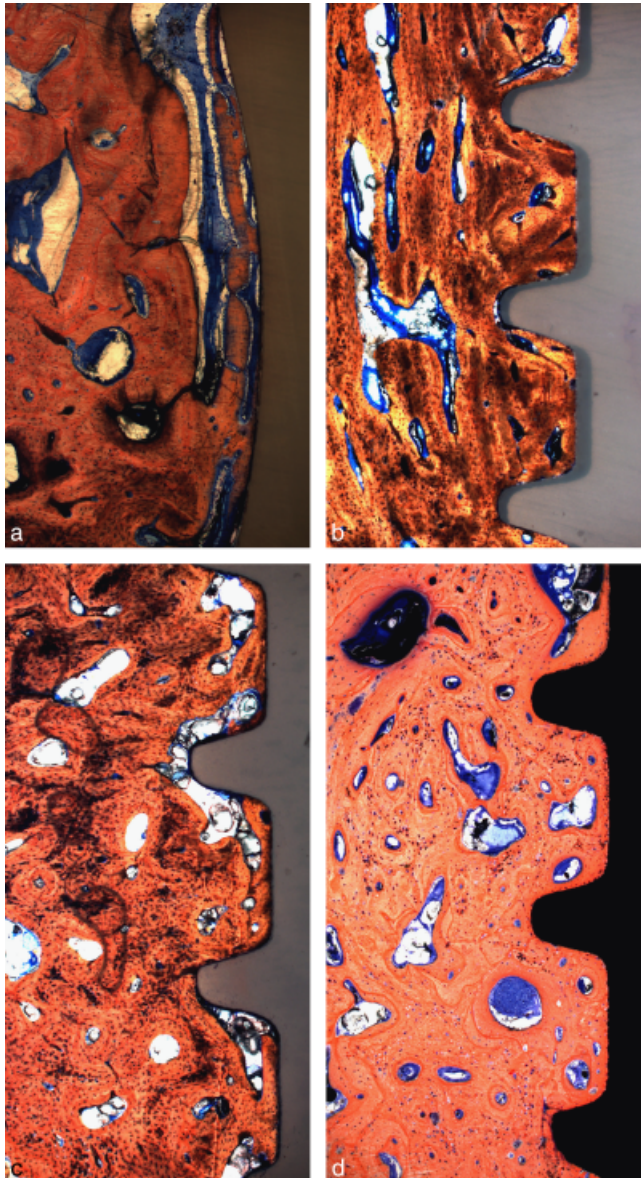


Fig. 5. (a) Micrograph showing osteoconductive bone formation after 13 weeks next to a sandblasted zirconia implant surface with small spots of bone implant contact (alizarine–methylene blue, original magnification $\times 150$). (b) Micrograph showing solid bone regeneration after 13 weeks next to a sandblasted zirconia implant (alizarine–methylene blue, original magnification $\times 50$). (c) Micrograph showing bone regeneration after 13 weeks adjacent to the sandblasted and etched surface of a zirconia implant. Thread tips appeared to be particularly devoid of bone (alizarine–methylene blue, original magnification $\times 50$). (d) Micrograph showing bone formation with high bone contact after 13 weeks adjacent to titanium implants (alizarine–methylene blue, original magnification $\times 50$).

(Palmieri et al. 2008) and alkaline phosphatase activity was significantly enhanced on the titanium surface over the zirconia surfaces (Hempel et al. 2010). However, Bächle and colleagues have reported similar proliferation of osteoblast-like cells on sandblasted and sandblasted/etched zirconia as well as sandblasted and acid-etched titanium surfaces (Bächle et al. 2007). The two surface modifications of zirconia

implants used in the present study had even shown significantly increased cell adhesion and proliferation on both zirconia surfaces compared with the sandblasted and acid-etched titanium surface (Hempel et al. 2010).

In the *in vivo* evaluation of these implant surfaces in the present study, the histologic features of early events of peri-implant bone regeneration suggest that bone formation on the surface of the

zirconia implants occurs in a slightly different manner than on the tested titanium surfaces. Osteoconductive bone formation on the implant surface appears to be enhanced on sandblasted and acid-etched titanium implants with thin and extensive layers of newly formed bone, whereas bone approached the zirconia implant surfaces with few spot-like contacts and an intervening non-mineralized tissue layer in some areas. The chemical analysis of the implant surfaces (XPS) did not show any unwanted residues and the overall carbon content was low. This indicates a clean implant surface (Buser et al. 2004) and suggests that different features in early peri-implant bone regeneration may be based on different characteristics of either surface roughness or surface chemistry and not on contaminations of the zirconia surface. Early events on the surface of biomaterials are based on the adsorption of proteins that enhance cell attachment, proliferation and differentiation. Adsorption of proteins is dependent on the surface charge, described by the isoelectric point (IEP) (Schliephake & Scharnweber 2008). Passive titanium oxide layers have been shown to have an IEP of 4.4 (Roessler et al. 2002), indicating that they carry a negative charge under *in vivo* conditions, whereas the IEP of zirconia has been determined to be around 7 (Leong et al. 1995, Kosmulski 2004), which implies a rather neutral surface charge under physiological pH conditions. Physisorption of positively charged proteins would therefore be more likely to occur on titanium surfaces than on zirconia surfaces. Additionally, the difference in the surface topography itself could have resulted in different contact angles and wettability and thereby may have contributed to the difference in osteoconductivity.

A significant difference between zirconia and titanium surfaces has also been found in the results of mechanical testing. The mean removal torque values have exhibited a clear superiority of titanium surfaces over both tested zirconia implants at both intervals. The findings are in line with those of a previous study that had tested a sandblasted and etched zirconia surface against sandblasted and acid-etched titanium surfaces (Ferguson et al. 2008). That study had shown that the mean removal torque was significantly lower for the zirconia surface than for the titanium surface after 4 and 8 weeks. The present

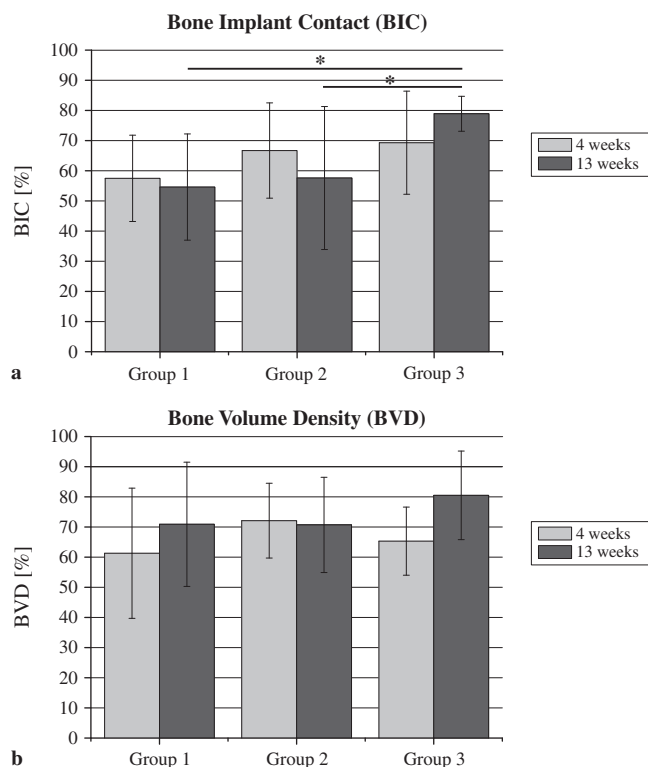


Fig. 6. (a) Bone to implant contact (BIC) after 4 and 13 weeks of implantation ($n = 6$). Statistically significant differences ($p < 0.05$) are indicated (*). (b) Bone volume density (BVD) after 4 and 13 weeks of implantation ($n = 6$). No statistically significant differences were observed.

results are also parallel to the report of Gahlert et al. (2007), who had found significantly reduced removal torque in zirconia implants with sandblasted surfaces compared with SLA titanium surfaces. When zirconia and titanium surfaces with similar surface roughness were compared ($S_a = 1.24$ and $1.30 \mu\text{m}$, respectively), comparable torque-out values were obtained (Sennerby et al. 2005). This would support the assumption that surface roughness does influence mechanical anchorage in bone to a higher degree than the material itself and that a zirconia surface with a comparable high surface roughness as the sandblasted and acid-etched titanium surface would achieve a comparable mechanical anchorage in bone.

The two zirconia surfaces showed an obvious difference in the failure mode during the torque-out test. The sandblasted and etched surface showed a clear breaking point, indicating a relatively brittle breakage, whereas no clear breaking point could be identified (Fig. 3, Type B) with the sandblasted zirconia implants. This may as well indicate an effect of interlocking of the surrounding bone with increased roughness of the implant surface. However, this observa-

tion could not be confirmed with the titanium implants, which showed both types of failure. Moreover, when the present sandblasted and etched implants were inserted into a different bone architecture in the iliac crest bone of sheep, a failure without a clear breaking point (Type B) was observed (Ferguson et al. 2008). Thus, interpretation of the type of failure with respect to all possible effects is still highly speculative on the basis of the present data.

The significantly worse mechanical performance of zirconia implants, however, appears to contradict the histomorphometric results of BIC after 4 weeks in the present study, where no difference was found with respect to peri-implant bone regeneration. The discrepancy between morphologic features and mechanical performance is difficult to interpret. One reason could be a direct mechanical effect of the difference in surface roughness. The higher surface roughness of the tested titanium surface in both the macro- and the microroughness range may lead to more intense interdigitation of bone, with the surface topography resulting in higher torque-out values. This interdigitation may not be appreciable on the light microscopic

level and may thereby result in significantly increased resistance against removal torque despite comparable morphometric results.

The same reason probably applies to the significant difference in removal torque between the two zirconia surfaces at 4 weeks, as the two surfaces showed a significant difference in both the micro- and the macroroughnesses, albeit lower than those with the control surface. The smaller difference in the roughness of the sandblasted and etched surface could then account for an increased mechanical interlocking during initial periods of osseointegration and hence an increased removal torque, which is levelled out at later intervals after 13 weeks. Moreover, residual alumina contamination from sandblasting might have additionally accounted for the difference in early bone anchorage.

Conclusion

The present study has shown that BIC of sandblasted and sandblasted/etched zirconia surfaces was comparable to sandblasted/etched titanium surfaces after 4 weeks but was significantly lower after 13 weeks due to a continued increase in BIC in the titanium group. Nevertheless, mechanical anchorage was significantly lower in both zirconia groups than titanium already after 4 weeks. It is hypothesized that this contradiction between the morphological and the mechanical results may be explained by increased mechanical interlocking of the titanium surface and adjacent bone due to its increased surface roughness. This interlocking effect appears to be below the resolution of conventional microscopy and, thus, is not appreciable by assessment of BIC rates.

Acknowledgements

The authors thank Dr. Roman Heuberger from the Robert Mathys Foundation in Bettlach for supporting them with XPS measurements.

References

- Akagawa, Y., Hosokawa, R., Sato, Y. & Kamayama, K. (1998) Comparison between freestanding and tooth-connected partially stabilized zirconia implants after two years' function in monkeys: a clinical and histologic study. *Journal of Prosthetic Dentistry* **80**, 551–558.

- Akagawa, Y., Ichikawa, Y., Nikai, H. & Tsuru, H. (1993) Interface histology of unloaded and early loaded partially stabilized zirconia endosseous implant in initial bone healing. *Journal of Prosthetic Dentistry* **69**, 599–604.
- Andriotelli, M., Wenz, H. J. & Kohal, R. J. (2009) Are ceramic implants a viable alternative to titanium implants? A systematic literature review. *Clinical Oral Implants Research* **20** (Suppl. 4), 32–47.
- Aparicio, C., Gil, F. J., Fonseca, C., Barbosa, M. & Planell, J. A. (2003) Corrosion behaviour of commercially pure titanium shot blasted with different materials and sizes of shot particles for dental implant applications. *Biomaterials* **24**, 263–273.
- Bächle, M., Butz, F., Hübner, U., Bakaliniš, E. & Kohal, R. J. (2007) Behavior of CAL72 osteoblast-like cells cultured on zirconia ceramics with different surface topographies. *Clinical Oral Implants Research* **18**, 53–59.
- Bornstein, M. M., Schmid, B., Belsler, U., Lussi, A. & Buser, D. (2005) Early loading of non-submerged titanium implants with a sand-blasted and acid-etched surface. 5-year results of a prospective study in partially edentulous patients. *Clinical Oral Implants Research* **16**, 631–638.
- Buser, D., Brogini, N., Wieland, M., Schenk, R. K., Denzer, A. J. & Cochran, D. L. (2004) Enhanced bone apposition to a chemically modified SLA titanium surface. *Journal of Dental Research* **83**, 529–533.
- Canullo, L. (2007) Clinical outcome study of customized zirconia abutments for single-implant restorations. *International Journal of Prosthodontics* **20**, 489–493.
- Ferguson, S. J., Langhoff, J. D., Voelter, K., von Rechenberg, B., Scharnweber, D. & Bierbaum, S. (2008) Biomechanical comparison of different surface modifications for dental implants. *International Journal of Oral and Maxillofacial Implants* **23**, 1037–1046.
- Fuerst, G., Gruber, R., Tangl, S., Sanroman, F. & Watzek, G. (2003) Enhanced bone-to-implant contact by platelet-released growth factors in mandibular cortical bone: a histomorphometric study in minipigs. *International Journal of Oral and Maxillofacial Implants* **18**, 685–690.
- Fuerst, G., Gruber, R., Tangl, S., Sanroman, F. & Watzek, G. (2004) Effects of fibrin sealant protein concentrate with and without platelet-released growth factors on bone healing of cortical mandibular defects. An experimental study in minipigs. *Clinical Oral Implants Research* **15**, 301–307.
- Gahlert, M., Gudehus, T., Eichhorn, S., Steinhäuser, E., Kniha, H. & Erhardt, W. (2007) Biomechanical and histomorphometric comparison between zirconia implants with varying surface textures and a titanium implant in the maxilla of miniature pigs. *Clinical Oral Implants Research* **18**, 662–668.
- Groessner-Schreiber, B., Hannig, M., Duck, A., Griepentrog, M. & Wenderoth, D. F. (2004) Do different implant surfaces exposed in the oral cavity of humans show different biofilm compositions and activities? *European Journal of Oral Sciences* **112**, 516–522.
- Grubbs, F. (1969) Procedures for detecting outlying observations in samples. *Technometrics* **11**, 1–21.
- Hempel, U., Hefti, T., Kalbacova, M., Wolf-Brandtstetter, C., Dieter, P. & Schlottig, F. (2010) Zirconia topography positively influences behaviour of osteoblasts-like SAOS-2 cells. *Clinical Oral Implants Research* **21**, 174–181.
- Jung, R. E., Sailer, I., Hämmerle, C. H., Attin, T. & Schmidlin, P. (2007) In vitro color changes of soft tissues caused by restorative materials. *International Journal of Periodontics and Restorative Dentistry* **27**, 251–257.
- Kohal, R. J., Wenig, D., Bächle, M. & Strub, J. R. (2004) Loaded custom-made zirconia and titanium implants show similar osseointegration: an animal experiment. *Journal of Periodontology* **75**, 1262–1268.
- Kokubo, Y., Tsumita, M., Sakurai, S., Torizuka, K., Vult von Steyern, P. & Fukushima, S. (2007) The effect of core framework designs on the fracture loads of all-ceramic fixed partial dentures on posterior implants. *Journal Oral Rehabilitation* **34**, 503–507.
- Kosmulski, M. (2004) pH-dependent surface charging and points of zero charge. II. Update. *Journal of Colloid and Interface Science* **275**, 214–224.
- Leong, Y. K., Scales, P. J., Healy, T. W. & Boger, D. V. (1995) Effect of particle size on colloidal zirconia rheology at the isoelectric point. *Journal of the American Ceramic Society* **78**, 2209–2212.
- Oliva, J., Oliva, X. & Oliva, J. D. (2007) One-year follow-up of first consecutive 100 zirconia dental implants in humans: a comparison of 2 different rough surfaces. *International Journal of Oral and Maxillofacial Implants* **22**, 430–435.
- Palmieri, A., Pezzetti, F., Brunelli, G., Muzio, L. L., Scarano, A. & Scapoli, L. (2008) Short-period effects of zirconia and titanium on osteoblast microRNAs. *Clinical Implant Dentistry and Related Research* **10**, 200–205.
- Park, S. E., Da Silva, J. D., Weber, H. P. & Ishikawa-Nagai, S. (2007) Optical phenomenon of peri-implant soft tissue. Part I. Spectrophotometric assessment of natural tooth gingival and peri-implant mucosa. *Clinical Oral Implants Research* **18**, 569–574.
- Piconi, C. & Maccauro, G. (1999) Zirconia as a ceramic biomaterial. *Biomaterials* **20**, 1–25.
- Rimondini, L., Cerroni, L., Carassi, A. & Torricelli, P. (2002) Bacterial colonization of zirconia ceramic surfaces: an in vitro and in vivo study. *International Journal of Oral and Maxillofacial Implants* **17**, 793–798.
- Roessler, S., Zimmermann, R., Scharnweber, D., Werner, C. & Worch, H. (2002) Characterization of oxide layers on Ti₆Al₄V and titanium by streaming potential and streaming current measurements. *Biointerfaces* **26**, 387–395.
- Rompen, E., Raepsaet, N., Domken, O., Touati, B. & Van Dooren, E. (2007) Soft tissue stability at the facial aspect of gingivally converging abutments in the esthetic zone: a pilot clinical study. *Journal of Prosthetic Dentistry* **97**, 119–125.
- Schliephake, H. & Scharnweber, D. (2008) Chemical and biological functionalization of titanium for dental implants. *Journal of Materials Chemistry* **18**, 2404–2414.
- Sennerby, L., Dasmah, A., Larsson, B. & Iverhed, M. (2005) Bone tissue responses to surface-modified zirconia implants: a histomorphometric and removal torque study in the rabbit. *Clinical Implant Dentistry and Related Research* **7**, 13–20.
- Stadlinger, B., Pilling, E., Huhle, M., Mai, M., Bierbaum, S. & Bernhardt, R. (2007) Influence of extracellular matrix coatings on implant stability and osseointegration: an animal study. *Journal of Biomedical Materials Research Part B: Applied Biomaterials* **83**, 222–231.
- Sundh, A. & Sjögren, G. (2008) A study of the bending resistance of implant-supported reinforced alumina and machined zirconia abutments and copies. *Dental Materials* **24**, 611–617.
- Wenz, H. J., Bartsch, J., Wolfart, S. & Kern, M. (2008) Osseointegration and clinical success of zirconia dental implants: a systematic review. *International Journal of Prosthodontics* **21**, 27–36.
- Whitehouse, D. J. (1994) *Handbook of Surface Metrology*, 1st edition. London: Taylor & Francis.
- Wieland, M., Textor, M., Spencer, N. D. & Brunette, D. M. (2001) Wavelength-dependent roughness: a quantitative approach to characterizing the topography of rough titanium surfaces. *International Journal of Oral and Maxillofacial Implants* **16**, 163–181.
- Zechner, W., Tangl, S., Fuerst, G., Tepper, G., Thams, U. & Mailath, G. (2003) Osseous healing characteristics of three different implant types. *Clinical Oral Implants Research* **14**, 150–157.

Address:

H. Schliephake

Department of Oral and Maxillofacial Surgery

George-Augusta-University

Robert-Koch-Str. 40

37075 Göttingen

Germany

E-mail: schliephake.henning@med.uni-goettingen.de

Clinical Relevance

Scientific rationale for study: Zirconia is considered to be an attractive material for dental implants because of its mechanical properties and its colour. The goal of this study was to examine the osseointegration of modified rough zirconia surfaces in

vivo compared with rough titanium surfaces.

Principal findings: The rough zirconia implants showed a lower degree of anchorage compared with the reference titanium implants. Lower peri-implant bone contact (BIC) and inferior mechanical anchorage was observed.

Practical implications: The tested zirconia surfaces achieve osseointegration. It is assumed that zirconia with rougher surfaces, comparable to the titanium surface tested, would achieve better mechanical anchorage and peri-implant bone attachment.

This document is a scanned copy of a printed document. No warranty is given about the accuracy of the copy. Users should refer to the original published version of the material.